

## Source distribution in interferometry for wave and diffusion

Yuanzhong Fan\* and Roel Snieder, Center for Wave Phenomena, Dept. of Geophysics, Colorado School of Mines, Golden CO 80401

### SUMMARY

For the wave equation, the Green's function that describes the waves propagating between two receivers can be reconstructed by cross-correlation if the receivers are enclosed by sources on a closed surface. This technique is normally called interferometry. The ordinary operator used in this technique is cross-correlation. The same technique for Green's function extraction can be applied to the solution of the diffusion equation if there are sources throughout in the volume. In practice, we only have a finite number of active sources. We address the question what minimum source density is needed for the accurate extraction of the Green's function, and how these sources should be located on the surface in the wave problem and if it is possible to reconstruct the Green's function of the diffusion equation by using a limited number of sources within a finite volume. We study these questions for homogeneous and isotropic media for both wave propagation and diffusion using numerical simulations. These simulations show that for the used model, the angular distribution of sources is critical in wave problems. For diffusion, the sensitivity of the sources decays away from the center of the two receivers. The required source distribution for early time and late time reconstruction is different.

### INTRODUCTION

In seismic imaging, the studies of interferometry and its applications have grown rapidly in recent years. Seismic interferometry in the exploration community is also referred to as the *virtual source method* (Bakulin and Calvert, 2004; Calvert et al., 2004; Bakulin and Calvert, 2006), and has been applied to imaging (Mehta et al., 2007; Vasconcelos et al., 2007). The sources used in this type interferometry can be either controlled shots (Bakulin and Calvert, 2004; Calvert et al., 2004; Schuster et al., 2004; Bakulin and Calvert, 2006; Mehta et al., 2007; van Wijk, 2006) or ambient noise (Weaver, 2005; Shapiro et al., 2005; Roux et al., 2005; Stehly et al., 2006; Godin, 2006; Curtis et al., 2006).

Interferometry applied to fields governed by the wave equation can be expressed, in the frequency domain, as (Snieder et al., 2007):

$$\begin{aligned} & G(\mathbf{r}_A, \mathbf{r}_B, \omega) - G^*(\mathbf{r}_A, \mathbf{r}_B, \omega) \\ &= \oint_S \frac{1}{\rho} (G^*(\mathbf{r}_A, \mathbf{r}, \omega) \nabla G(\mathbf{r}_B, \mathbf{r}, \omega) \\ &\quad - (\nabla G^*(\mathbf{r}_A, \mathbf{r}, \omega)) G(\mathbf{r}_B, \mathbf{r}, \omega)) \hat{\mathbf{n}} dS, \end{aligned} \quad (1)$$

where  $G(\mathbf{r}_A, \mathbf{r}_B, \omega)$  is the displacement Green's function that describes wave propagation from receiver at  $\mathbf{r}_B$  to the receiver at  $\mathbf{r}_A$  respectively, \* indicates complex conjugation,  $G(\mathbf{r}_A, \mathbf{r}, \omega)$  and  $G(\mathbf{r}_B, \mathbf{r}, \omega)$  are the Green's functions that describe waves

received by receiver A and B from a source at position  $\mathbf{r}$ ,  $S$  is the surface where sources are located,  $\hat{\mathbf{n}}$  is the unit vector perpendicular to the surface  $dS$ ,  $\omega$  is the angular frequency,  $\rho$  is the density and  $c$  is the medium velocity. When the waves satisfy a radiation boundary condition on the surface  $S$ ,

$$\nabla G(\mathbf{r}_A, \mathbf{r}, \omega) \approx i(\omega/c) G(\mathbf{r}_A, \mathbf{r}, \omega) \hat{\mathbf{r}},$$

equation (1) becomes

$$\begin{aligned} & G(\mathbf{r}_A, \mathbf{r}_B, \omega) - G^*(\mathbf{r}_A, \mathbf{r}_B, \omega) \\ &\approx \frac{2i\omega}{\rho c} \oint_S G(\mathbf{r}_A, \mathbf{r}, \omega) G^*(\mathbf{r}_B, \mathbf{r}, \omega) (\hat{\mathbf{r}} \cdot \hat{\mathbf{n}}) dS, \end{aligned} \quad (2)$$

In the time domain, equation (2) states that integrating the cross correlation of wave fields at receivers A and B from one source over the surface  $S$  and taking the time derivative of it, we obtain the response between the two receivers where one of them acts as a source. In addition to the causal response  $G$ , we also retrieve the time-reverse  $G^*$  of this response.

The expression for Green's function extraction for fields governed by the diffusion equation is similar to that for waves. The main difference is that the surface integral becomes a volume integral (Snieder, 2006b):

$$\begin{aligned} & G(\mathbf{r}_A, \mathbf{r}_B, \omega) - G^*(\mathbf{r}_A, \mathbf{r}_B, \omega) \\ &= 2i\omega \int_V G(\mathbf{r}_A, \mathbf{r}, \omega) G^*(\mathbf{r}_B, \mathbf{r}, \omega) dV, \end{aligned} \quad (3)$$

in which  $V$  is the volume containing the sources. The meaning of other terms are the same as those in equation (2).

Equations (2) and (3) show that the main difference between wave and diffusion interferometry is the required source distribution. For waves, equation (2) shows that if two receivers are surrounded by active sources on a closed surface, the response which describes the wave propagating between the two receivers can be reconstructed as if one of the receivers were an active source. For diffusion, equation (3) states that the sources are required to be everywhere in the volume (Snieder, 2006b). In practice, there are only a finite number of sources. Therefore, we can never have a closed source surface for waves or sources throughout the volume for diffusion. This raises the question: what is the required source density and how should we locate these sources in order to reconstruct the Green's function accurately?

The importance of cross-correlation-based interferometry for waves has been addressed by numerous authors. On the other hand, cross-correlation-based interferometry for diffusion is still at the theory stage and there are no field applications yet. In exploration geophysics, there are at least two important diffusive fields: pore pressure and low-frequency inductive electromagnetic fields. From the pore pressure we can infer the fluid conductivity between wells (Voyiadjis and Song, 2003;

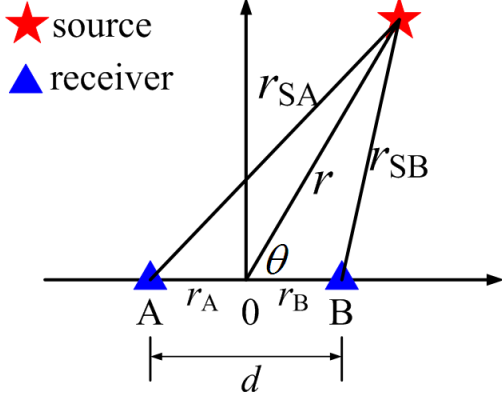


Figure 1: Definition of the source radius  $r$  and source angle  $\theta$  that define a source position in 2-D.

Nokken and Hooton, 2007). Electromagnetic fields carry information about the resistivity of the pore fluid and may thus help distinguish between hydrocarbons and water. For the offshore oil exploration, controlled-source electromagnetic (CSEM) is one of the most important techniques used to detect hydrocarbon (Hoversten et al., 2006; Constable and Srnka, 2007; Darnet et al., 2007; Scholl and Edwards, 2007).

## MODEL AND RESULTS

### Waves

For simplicity, we use a 2-D homogeneous model, with constant velocity 1 km/s, in the numerical tests. For defining the source position, we use two parameters: source angle and source radius as shown in Figure 1. A and B are two receivers with a separation  $d$ . The position vectors of the two receivers are denoted by  $\mathbf{r}_{SA}$  and  $\mathbf{r}_{SB}$ , respectively. The source function for waves we use in all the examples in this paper is a Ricker wavelet with a central frequency of 0.5 Hz. The source amplitude is the same for all sources.

### Experiment 1: uniformly distributed source angle.

We first study the effect of the source angle distribution. Sources are uniformly distributed on the circle with a radius of 40 km. The distance between the two receivers is 6 km. Figure 2 shows the reconstructed response between the two receivers for a homogeneous distribution of sources with increasing number of sources. The response has two parts, the causal and anti-causal parts as represented by equation (2). If we replace one of the receivers with an active source, the received signal arrives after a propagation time of 6 s. To make the shape of the received signal the same as the reconstructed signal, we correlate the received signal with the source-time function. This new signal is represented by the dashed line in the bottom panel, it is virtually the same as the causal part of the reconstructed response with 50 sources (the amplitudes of both reconstructed and active signals are normalized).

We quantify the spurious fluctuations that arrive between the

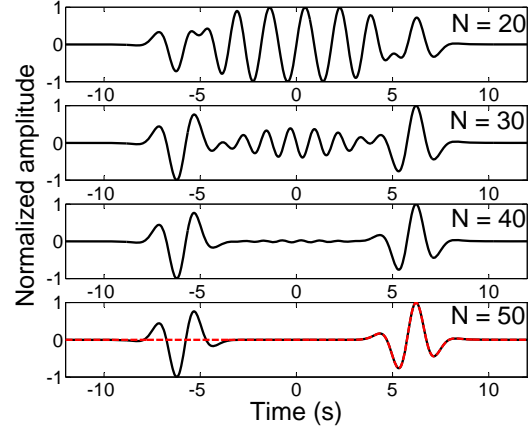


Figure 2: Reconstructed responses for uniform angle distribution with different number of source  $N$  (the dashed line in the bottom panel is the exact response between the two receivers)

anti-causal and the causal response by defining the fluctuation energy

$$E_m = \frac{1}{N_m} \sum_{i=1}^{N_m} A[i]^2, \quad (4)$$

in which  $N_m$  is the number of discrete sample points in the middle part of the signal, i.e. the part between the two main pulses. Weaver and Lobkis (2005) showed that these fluctuations decay as  $N^{-1}$  if the sources are randomly distributed. Our study shows when the source angles are uniformly distributed, the decay rate of  $E_m$  is even faster than  $N^{-10}$ .

### Experiment 2: randomly distributed source angle.

In this experiment, the source angles are randomly distributed while the source radius is constant. Figure 3 shows the reconstructed response as a function of number of sources  $N$  for a random distribution of sources along the circle. Compared with figure 2, the random distribution gives a much poorer reconstruction than does the uniform distribution with the same number of sources. The fluctuation energy  $E_m$  decay behavior is consistent with the prediction of Weaver and Lobkis(2005): the decay is proportional to  $N^{-1}$ . Experiment 2 suggests that not only the number of the source is important, but also their angular distribution.

### Experiment 3: source radius importance.

In the previous two experiments we learned how the angle distribution influences the response extraction. There is, however, still another parameter: the radius  $r$  as defined in figure 1. In the next example we compare the result from two distributions with the same angle distribution but different source radii. The first one is the example we showed in experiment 1, where 50 sources are uniformly distributed on a circle (stars in the upper panel of figure 4). The second one is for sources with the same angle distribution but the radius is randomly varying in a range

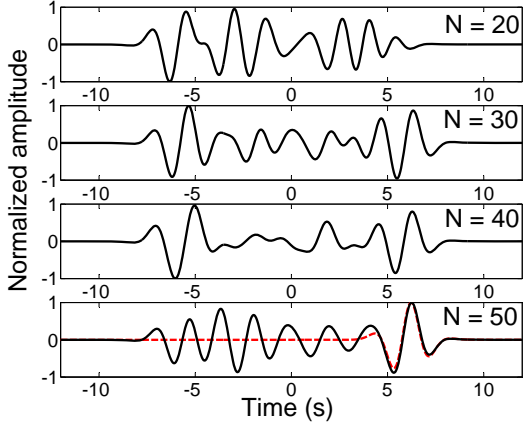


Figure 3: Reconstructed responses for random angle distribution with different number of sources  $N$  (the dashed line in the bottom panel is the exact response between the two receivers).

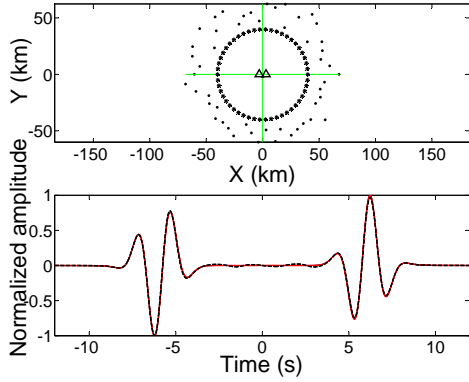


Figure 4: Two source distributions with the same angle distribution but different radii (top) and the reconstructed responses: red solid (same radius), black dashed line (different radius)

in which all radii are much larger than the distance between the two receivers (dots in the upper panel of figure 4). The reconstructed responses in figure 4 suggest that varying the source radii does not degrade the accuracy of the Green's function extraction. This is only true when source radii are much larger than the distance between the two receivers.

### Diffusion

Equation (3) shows that sources in the whole volume are needed to extract the Green's function for diffusion. To simplify the problem, we show a numerical test in a 1-D medium with constant diffusion coefficient. The same strategy can also be extended to a 3-D model with constant diffusion coefficient. We choose the origin of the coordinate system at the center of the two receivers. The distance between the two receivers is 2 km. The diffusion coefficient used in this model is  $D = 1 \text{ km}^2/\text{s}$ .

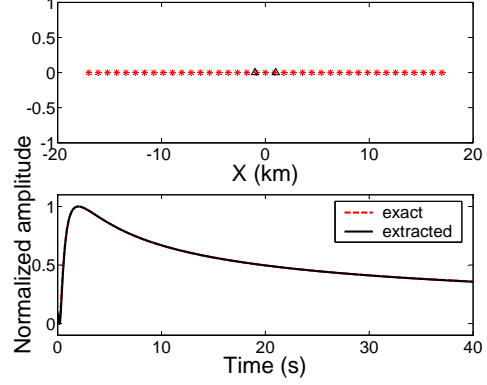


Figure 5: 1-D source distribution with  $W_s = 34 \text{ km}$ ,  $\rho_s = 1.147 \text{ km}^{-1}$  and the extracted Green's function.

$W_s$  is the width of the distribution (distance from the most-left source to the most-right source) and  $\rho_s = N/W_s$  is the source density. Figure 5 shows an accurate reconstruction with a required source distribution. The early-time reconstruction is controlled by the source density  $\rho_s$  and late-time reconstruction is more affected by the distribution width  $W_s$  (The early time response is defined as the response before the peak in the Green's function of the diffusion equation, the late time part is defined as the response after the main peak).

## DISCUSSION/CONCLUSIONS

### Waves

The Green's function of the wave equation in 2D is represented in the frequency domain by the first Hankel function of degree zero. In all the numerical simulations in this paper, we use the far field approximation:

$$G(r) = \sqrt{\frac{1}{8\pi kr}} e^{i(kr + \pi/4)}. \quad (5)$$

Inserting this into equation (2) with far field assumptions  $r_{SA} \approx r_{SB} \approx r$ ,  $r_{SA} - r_{SB} \approx d \cos \theta$  and  $\hat{r} \cdot d\vec{S} = r d\theta$ , we obtain

$$G(\mathbf{r}_A, \mathbf{r}_B, \omega) - G^*(\mathbf{r}_A, \mathbf{r}_B, \omega) \approx \frac{i}{4\pi\rho} \int_0^{2\pi} e^{ikd \cos \theta} d\theta \quad (6)$$

Note that the right hand side does not depend on the source radius  $r$ . Experiment 3 in the wave part supports this conclusion: in that experiment, variations in the source radius do not influence the Green's function extraction.

The right hand side of equation (6) is the integral representation of the Bessel function (Snieder, 2006a), which is related to the exact Green's function:

$$\begin{aligned} \frac{1}{2\pi} \int_0^{2\pi} e^{ikd \cos \theta} d\theta &= J_0(kd) \\ &= \frac{1}{2} (H_0^{(1)}(kd) - H_0^{(1)}(-kd)) \end{aligned} \quad (7)$$

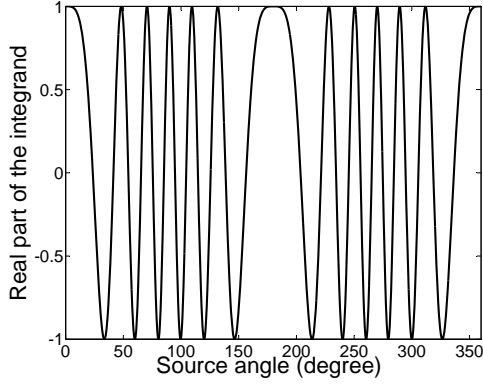


Figure 6: The real part of the integrand in equation (6).

This shows that by using only far field of the waves in the interferometry, both far field and near field response are reconstructed. For the dependence on the angle  $\theta$ , we need to study the character of the integrand in equation (6). The real part of this integrand is the oscillatory function shown in figure 6. The extraction of the Green's function depends on the sampling of this integral over source angle  $\theta$ , and reduces to the numerical integration of a continuous oscillatory function. The derived minimum required source density if the sources are uniformly distributed in a homogeneous medium is:

$$\rho_s = 0.4kd \text{ (radian}^{-1}\text{)}, \quad (8)$$

We also test different source distribution for an heterogeneous medium with 200 point scatters. Taking all the multiple scattered waves into account, the uniform source angle distribution still gives much more accurate reconstruction.

In conclusion, for wave interferometry in a homogeneous model, the most important parameter is the source angle distribution. Uniform angle distribution is the best to reconstruct the response accurately. If randomly distributed sources are used, much larger number of sources are needed to have accurate reconstruction. This conclusion holds when all sources have the same amplitude. If the amplitude of the sources fluctuates randomly, a uniform angle distribution gives similar reconstruction of the Green's function as the random angle distribution for a constant source strength.

### Diffusion

The frequency domain Green's function of the diffusion equation in a 1-D homogeneous medium is given by

$$G(x, \omega) = \frac{1}{(1+i)\sqrt{2\omega D}} e^{(-1-i)x\sqrt{\omega/2D}} \quad (9)$$

Inserting this expression into equation (3), gives

$$\begin{aligned} & G(\mathbf{r}_A, \mathbf{r}_B, \omega) - G^*(\mathbf{r}_A, \mathbf{r}_B, \omega) \\ &= \frac{i}{2D} \int_x e^{-(r_{SA}+r_{SB})\sqrt{\omega/2D}} e^{-i(r_{SA}-r_{SB})\sqrt{\omega/2D}} dx \end{aligned} \quad (10)$$

Similar as for the analysis of the wave, we study the real part of the integrand of equation (10) as a function of space vari-

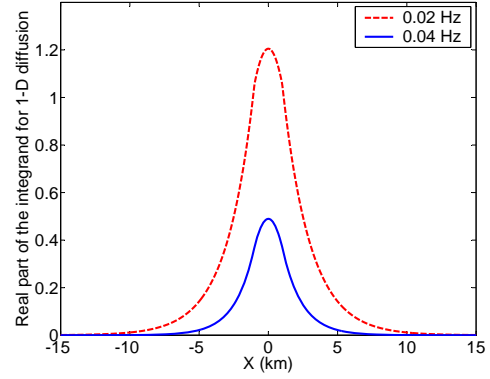


Figure 7: The real part of the integrand in equation (10) at two different frequencies.

able  $x$ . Notice that the integrand is also a function of frequency  $\omega$ . Therefore, for different frequencies the real part of the integrand behaves differently. Figure 7 shows this integrand for two different frequencies. The width of the distribution decreases with frequency. Quantitatively we can conclude that because the early time behavior of the Green's function has more high frequency components, the required source distribution can be narrower. With small  $W_s$ , the early time behavior is reconstructed well. With increasing  $W_s$ , more lower frequency components are recovered. Since the tail of the Green's function mostly contains low frequencies, Green's function of late time is recovered accurately with a large width  $W_s$ . Consequently, the source density  $\rho_s$  controls the retrieval of the high frequency components of the Green's function (eg. early time of the Green's function), and the width of the distribution  $W_s$  controls lower frequency components (eg. the late time of the Green's function).

We derive the minimum source distribution width for accurate reconstruction up to time  $\tau_a$  is:

$$W_s = 4\sqrt{D\tau_a} + d \quad (11)$$

The minimum source density for the accurate early-time reconstruction is

$$\rho_s = 2\sqrt{\omega/2D} \quad (12)$$

In conclusion, for cross-correlation-based diffusion interferometry, instead of having sources everywhere in the volume, it suffices to have sources in only a small volume surrounding the receivers as shown in figures 7. For the 1-D problem, the source distribution width controls the late-time (low-frequency components) reconstruction of the Green's function and source density controls the early-time (high-frequency components) reconstruction.

### ACKNOWLEDGMENTS

The authors would like to thank the CWP sponsors and colleagues for their supports and Shell GameChanger program.

## REFERENCES

- Bakulin, A. and R. Calvert, 2004, Virtual source: new method for imaging and 4D below complex overburden: SEG Technical Program Expanded Abstracts, **23**, 2477–2480.
- , 2006, The virtual source method: Theory and case study: *Geophysics*, **71**, SI139–SI150.
- Calvert, R., A. Bakulin, and T. Joners, 2004, Virtual sources, a new way to remove overburden problems: Expanded abstracts of the 2004 EAEG-meeting, 2477–2480.
- Constable, S. and L. J. Srnka, 2007, An introduction to marine controlled-source electromagnetic methods for hydrocarbon exorption: *Geophysics*, **72**, WA3–WA12.
- Curtis, A., P. Gerstoft, H. Sato, R. Snieder, and K. Wapenaar, 2006, Seismic interferometry-turning noise into signal: *The Leading Edge*, **25**, 1082–1092.
- Darnet, M., M. C. K. Choo, R. E. Plessix, M. L. rosenquist, K. Yip-Cheong, E. Sims, and J. W. K. Voon, 2007, Detecting hydrocarbon reservoirs from CSEM data in complex setting: Application to deepwater Sabah, Malaysia: *Geophysics*, **72**, WA97–WA103.
- Godin, O. A., 2006, Recovering the acoustic Green's function from ambient noise cross correlation in an inhomogeneous moving medium: *Phys. Rev. Lett.*, **97**, 054301–4.
- Hoversten, G. M., G. A. Newman, N. Geier, and G. Flanagan, 2006, 3D modeling of a deepwater EM exploration survey: *Geophysics*, **71**, G239–G248.
- Mehta, K., A. Bakulin, J. Sheiman, R. Calvert, and R. Snieder, 2007, Improving the virtual source method by wavefield separation: *Geophysics*, **72**, V79–V86.
- Nokken, M. R. and R. D. Hooton, 2007, Using pore parameters to estimate permeability or conductivity of concrete: *Materials and Structures*, **41**, 1–16.
- Roux, P., K. G. Sabra, W. A. Kuperman, and A. Roux, 2005, Ambient noise cross correlation in free space: Theoretical approach: *J. Acoust. Soc. Am.*, **117**, 79–84.
- Scholl, C. and R. N. Edwards, 2007, Marine downhole to seafloor dipole-dipole electromagnetic methods and the resolution of resistive targets: *Geophysics*, **72**, WA39–WA49.
- Schuster, G. T., J. Yu, J. Sheng, and J. Rickett, 2004, Interferometric/daylight seismic imaging: *Geophys. J. Int.*, **157**, 838–852.
- Shapiro, N. M., M. Campillo, L. Stehly, and M. H. Ritzwoller, 2005, High-resolution surface-wave tomography from ambient seismic noise: *Science*, **307**, 1615–1618.
- Snieder, R., 2006a, *A guided tour of mathematical methods: For the physical sciences*: Cambridge University Press, 2 edition.
- , 2006b, Retrieving the Green's function of the diffusion equation from the response to a random forcing: *Phys. Rev. E*, **74**, 046620.
- Snieder, R., K. Wapenaar, and U. Wegler, 2007, Unified greens function retrieval by cross-correlation; connection with energy principles: *Phys. Rev. E.*, **75**, 036103.
- Stehly, L., M. Campillo, and N. M. Shapiro, 2006, A study of seismic noise from its long-range correlation properties: *J. Geophys. Res.*, **111**, B10306.
- van Wijk, K., 2006, On estimating the impulse response between receivers in a controlled ultrasonic experiment: *Geophysics*, **71**, SI79–SI84.
- Vasconcelos, I., R. Snieder, and B. Hornby, 2007, Target-oriented interferometry — imaging with internal multiples from subsalt VSP data: SEG Technical Program Expanded Abstracts, **26**, 3069–3073.
- Voyiadjis, G. Z. and C. R. Song, 2003, Determination of hydraulic conductivity using Piezocone penetration test: *Int. J. Geomech.*, **3**, 217–224.
- Weaver, R. L., 2005, Information from seismic noise: *Science*, **307**, 1568–1569.
- Weaver, R. L. and O. I. Lobkis, 2005, Fluctuations in diffuse field-field correlations and the emergence of the Green's function in open systems: *J. Acoust. Soc. Am.*, **117**, 3432–3439.